Journal of Building Engineering 76 (2023) 107060

Contents lists available at ScienceDirect

Journal of Building Engineering

journal homepage: www.elsevier.com/locate/jobe

Mechanical, natural and hybrid ventilation systems in different building types: Energy and indoor air quality analysis

Giacomo Tognon *, Marco Marigo, Michele De Carli, Angelo Zarrella

Department of Industrial Engineering - Applied Physics Section, University of Padova, Via Venezia 1, 35131, Italy

ARTICLE INFO

Keywords:
Air conditioning systems
Hybrid ventilation
Natural ventilation
Infection risk
Building simulations

ABSTRACT

Ventilation is fundamental for providing good Indoor Air Quality in buildings. Nevertheless, it involves considerable energy consumption. In this paper, a co-simulation approach was applied to two case studies, a residential and an educational building, to evaluate different control strategies for hybrid ventilation systems in terms of annual energy demand and risk mitigation. The simulations were performed using TRNSYS and CONTAM and successively applying the Wells-Riley model to estimate the airborne infection risk. The analysis is performed for three climates, Venice, Rome and Helsinki. Results for the apartment show that different control strategies do not lead to significant variations in the overall heating demand for a given climate. In contrast, increasing natural ventilation hours during the cooling season produces savings in both sensible (up to 31% in Venice) and latent demand (up to 30% in Rome). Fan absorption in the heating season is reduced by 40% and 86% in Rome for the flat and classroom, respectively and by 84% in Venice for the apartment in the cooling season. Moreover, a control strategy enhancing natural ventilation is promising in reducing the infection risk. Therefore, if well-regulated through a suitable control strategy, the hybrid ventilation system seems promising in maintaining healthy indoor environments while reducing energy consumption.

List of symbols

ACH	Air Changes per Hour [h^{-1}]
C	Quanta concentration [quanta m^{-3}]
c_p	Specific heat at constant pressure [J kg^{-1} K^{-1}]
E	Annual Energy use [kWh]
ER	Quanta emission rate [quanta h^{-1}]
H	Height [m]
h	Enthalpy [kJ kg^{-1}]
I	Number of infected sources [−]
k	Loss term for gravitational deposition [h^{-1}]
$\dot{m}$	Mass flow rate [kg s^{-1}]
P_I	Airborne infection probability [%]
p	Breathing flow rate [m^3 h^{-1}]

* Corresponding author.
E-mail address: giacomo.tognon.2@studenti.unipd.it (G. Tognon).

https://doi.org/10.1016/j.jobe.2023.107060
Received 23 March 2023; Received in revised form 24 May 2023; Accepted 9 June 2023
Available online 10 June 2023

q	Power [kW]
$r_{0,\,w}$	Latent heat of vaporization of water (at 0°C) [kJ kg^{-1}]
t	Time [h]
V	Room Volume [m^3]
W	Width [m]
x	Specific humidity [kg kg^{-1}]
λ	Loss term for viral inactivation [h^{-1}]
τ	Timestep length [s]
ΔT_{lim}	Temperature difference threshold [°C]

Subscripts/superscripts

AH	Air handling
cool	Cooling season
CD	Cooling and dehumidification process
da	Dry air
el	Electrical
ext	External environment
heat	Heating season
in	Indoor environment
lat	Latent
M	Mid-season
postH	Post-heating process
preH	Pre-heating process
sens	Sensible
v	Vapor

Acronyms/abbreviations

LR	Living Room
MB	Master Bedroom
MV	Mechanical Ventilation
NV	Natural Ventilation
SB	Single Bedroom
TRY	Test Reference Year

1. Introduction

The statistics reported by Eurostat [1] show that the building sector has significantly impacted final energy consumption in recent years. In 2020, the final energy use in residential, commercial, and public sectors in EU countries was estimated to be 42% of the total. For this reason, issues concerning energy savings in buildings are increasing in importance nowadays. A significant amount of energy is used every day to ensure good quality of life in the enclosed environment. In particular, with the recent spread of the COVID-19 pandemic, public attention has been focused on the issue of indoor air quality (IAQ), particularly on virus transmission and indoor environmental healthiness. According to the World Health Organization (WHO) [2], the transmission of the SARS-CoV-2 virus takes place through both a direct transmission and an indirect or airborne transmission route [3]. It has been widely recognized that airborne transmission played a crucial role during the pandemic [4], and the search for solutions converged on ventilation as an effective strategy to mitigate infection risk [5]. However, its implementation in new and existing buildings is not trivial. Mechanical ventilation systems are very efficient in controlling the IAQ, but their use involves increased energy consumption that cannot be overlooked. For this reason, a holistic approach to the issue is recommended in the literature, taking into consideration the maximization of indoor air quality and cost minimization [6]. A promising solution that can contribute to this topic is the hybrid ventilation approach studied in detail by Annex 35 of the International Energy Agency (IEA) [7]. Its purpose is to provide good IAQ in buildings through the combination of natural ventilation and mechanical systems. In the existing literature, many authors reported about measurements in naturally ventilated buildings such as classrooms in UK [8], in Chinese residential buildings [9] and Spanish homes [10]; in all these papers, an appropriate use of natural ventilation is observed to be sufficient for guaranteeing good indoor pollutants' concentration level, but to keep good thermal comfort standards, they suggest to adopt hybrid ventilation strategies. This solution is widely studied in the literature and is applied in the so-called "mixed-mode buildings" [11]. When monitoring environments with hybrid strategies, the thermal comfort result to be enhanced, with a good control of indoor pollutants concentration [12]. To reach these results, the control system is designed to find a trade-off between minimizing costs and maximizing IAQ [13]. In many works, the potential of savings of hybrid ventilation systems is reported: according to Chen et al., up to 50% of energy can be saved [14]; however, it is also well-known that this scenario is possible only with a well-built control system. Cho et al. [15] propose a "humidity sensitive" control system for indoor air flows, coupled with a hybrid ventilation system with switching control based on outdoor air temperature and wind speed

ranges. Vallianos et al. [16] compare a reference control system based on fixed ranges of outdoor temperature and humidity with a reactive and a predictive control system, highlighting the higher thermal comfort and energy savings of the latter solution. In their paper, Menassa et al. [17] focus on the scheme of a control system for hybrid ventilation solutions, and its layout is divided into four parts, each one verifying if the corresponding variable (e.g., temperature, humidity, energy consumption, CO_2 concentration) is at a suitable level for enabling natural instead of mechanical ventilation. Less et al. [18] analysed six control strategies for hybrid ventilation with co-simulation in CONTAM and Energy Plus for different residential buildings in California. They found that the best control strategies could save up to 50% on energy-related ventilation, maintaining good air quality. Park et al. [19] evaluated some scenarios of extending the natural ventilation period in hybrid ventilated buildings in Korea using EnergyPlus. They concluded the possibility of energy savings between 32% and 34% for their case study. Finally, Vadamalraj et al. [20] presented a novel hybrid ventilation system controlled with model predictive control (MPC) algorithms and soft sensors. Its application in laboratory tests highlighted good thermal comfort and IAQ levels with energy savings of 19–21% compared to the case without its implementation. O'Donovan and O'Sullivan focus on design stage and study different ventilation approaches, suggesting the employment of hybrid solutions for the simultaneous control of thermal comfort and virus transmission [21]. An important contribution to the hybrid ventilation modelling is given by Stasi et al., who simulated with the EnergyPlus software three different hybrid ventilation strategies in an NZEB building for different Italian climates [22]. A significant contribution to this type of ventilation system analysis comes from building simulations. They are widely used in energy consumption evaluations and IAQ assessments, and the purpose of the simulation approach is to compare solutions or predict different scenarios. Among all the simulation software, TRNSYS [23] is used for the simulation of dynamic models, especially for the analysis of building energy systems; CONTAM [24] is a widely employed tool for the computational analysis of ventilation and indoor air quality (IAQ) in multi-zonal models of buildings. Both TRNSYS and CONTAM have been already validated in previous works [25,26], and they are now consolidated and widely used software in the field of building simulations. Their high flexibility allows a co-simulation approach in which the thermal and ventilation model solutions use each other for a multi-domain approach. For this reason, different papers in the literature use the coupling of these two programs to evaluate the impact of natural ventilation on energy consumption and indoor temperatures [27–29]. Wen et al. developed an integrated TRNSYS-CONTAM model to study the energy performance of a multi-energy system combining hybrid ventilation, a ground-source heat pump (GSHP), and photovoltaic thermal (PVT) collectors [30] Picard et al. studied coupled CONTAM to TRNSYS to assess the airborne transmission of SARS-CoV-2 in a typical detached house where an exhaust mechanical ventilation system is installed [31]. Pistochini et al. studied the mechanical ventilation inside classrooms with a focus on filtering and economizer effect on energy use and infection risk with the Wells-Riley model [32].

To the best of authors' knowledge, there is no evidence in the literature of previous works applying a co-simulation approach with the TRNSYS-CONTAM software for the evaluation of hybrid ventilation systems looking at both energy demand and air salubrity. Therefore, this paper proposes the integration of TRNSYS with CONTAM for the development of a dynamic simulation building model to analyse hybrid ventilation strategies in two case studies: a seven-thermal zone-residential building and a typical school classroom. In this way, the calculation of the energy consumption considering both mechanical and natural ventilation during the building management is allowed. Moreover, the literature search revealed the lack of an integrated analysis of energy and salubrity aspects related to hybrid ventilation use in indoor environments. For this reason, a further analysis is carried out with the Wells-Riley model [33,34] to assess the airborne infection risk from COVID-19 inside the occupied space. A control strategy based on occupancy and external temperature is implemented for the ventilation system operation, and a simulation approach is adopted to study different scenarios related to the set control parameters. The objective is investigating how the control system affects both the energy demand and the virus transmission. From this point of view, the paper proposes a comprehensive approach for the assessment of hybrid ventilation effectiveness, and the comparison between different scenarios using this method is enhanced.

2. Methodology

The analysis of a hybrid ventilation system was carried out considering a residential building and a school classroom. A dynamic simulation building model was built exploiting the coupling process between TRNSYS and CONTAM. Both simulation platforms apply a multi-zonal approach to model the building spaces. TRNSYS performed the dynamic energy simulation, determining the net energy demand for heating and cooling purposes of internal conditioned spaces, and zones' temperatures. CONTAM was applied to define a multi-zonal ventilation model to calculate infiltrations from the external environment driven by natural ventilation forces and air couplings between adjacent zones.

2.1. Case studies

Two different case studies were simulated with the model described in the following sections: a two-story residential apartment and a school classroom. The flat is a portion of a multi-family house with four occupants, adjacent to other flats on the lower floor and two sides. Two sidewalls (North and South oriented) and the roof face the external environment. The apartment comprises seven thermal zones: a living room with a kitchen, two bedrooms, two bathrooms, a passageway and a stairwell. The school classroom is modelled as a single thermal zone with one wall facing the outside (East oriented), whereas all the others are adjacent to heated indoor environments. In the apartment case, thermal transmittances of 0.34 and 0.3 W/(m^2 K) were employed for external walls and roof covering slab, respectively, according to Ref. [35]. On the other hand, thermal transmittance of 0.5 W/(m^2 K) was assumed for classroom opaque external surfaces. In both cases, glazed surfaces with a transmittance of 2.2 W/(m^2 K) were considered. The main geometrical characteristics of the case studies are reported in Table 1.

For both cases, the simulations are performed in three locations: Helsinki, Venice and Rome. Therefore, the climate conditions for

Table 1
Case studies characteristics.

	Floor Area [m^2]	Net Heated Floor Area [m^2]	Floor height [m]	External opaque surface [m^2]	External glazed surface [m^2]
Residential Apartment	75.7	58.4	2.7	98.7	14.9
School Classroom	48.0	48.0	3.0	24.0	8.6

the model were obtained from the Test Reference Year (TRY) of these cities, from the EnergyPlus database [36].

2.2. Airflow network model for natural ventilation

The overall model of the analysed case studies can be split into two parts: a multizone ventilation model and a transient thermal model. The first one consists of the building airflow network created with CONTAM. Fig. 1 outlines the ventilation model of the residential building and the adopted zoning. Relative elevation, height and dimensions of windows, doors and vents are representative of a real naturally ventilated building located in Vigonza, a town between Padua and Venice (Italy). Doors are included in the model, but they are assumed to be always closed. However, the airflow paths through small gaps placed around the door perimeter are modelled as leakage elements of 80 cm^2 for each internal door and 50 cm^2 for the entrance door. A power law links the air flow rate with the pressure gradient across the gaps, and a discharge coefficient and a flow exponent of 0.6 and 0.65 were assumed, respectively [24]. Stair doorways are considered like two big rectangular openings in the walls separating the stairwell from the connected spaces.

Bathrooms are linked to adjacent zones through two vents near the ceiling to promote the extraction of air from those zones and its successive expulsion. These openings are modelled as orifices with a cross-sectional area of 40 cm^2; a discharge coefficient of 0.6 and a flow exponent of 0.5 were set as power law parameters [24]. Windows are designed the same way as doors, with a leakage area of 30 cm^2; nevertheless, their upper part is assumed to be openable and the opening area can be adjusted by a factor ranging between 0 and 1. The top-hung devices are modelled as a "two-way" flow path since a bidirectional airflow may occur for larger flow elements. The geometrical characteristics of these elements are outlined in Table 2. Finally, the second-floor bathroom is linked to the external environment through a roof solar chimney [37]. It is modelled as an orifice at 2.20 m above the bathroom ceiling with the same fluid dynamic properties of bathrooms' vents and a free flow area of 0.80 m^2. Wind effect on airflows through external openings was also considered by providing a set of pressure coefficients for the whole building. Their value is based upon the relative orientation between the wall where the window is installed and wind direction, following the model of Swami and Chandra for low-rise buildings [38]. The classroom is modelled as a single thermal zone connected to the external environment through three windows (East oriented) with dimensions of 1.9 m x 1.5 m. As for the apartment, they are kept close with a leakage area of 30 cm^2 and a top hung element is placed with a variable opening degree. The openable upper part of the fixture is 0.6 m high and 1.5 m wide.

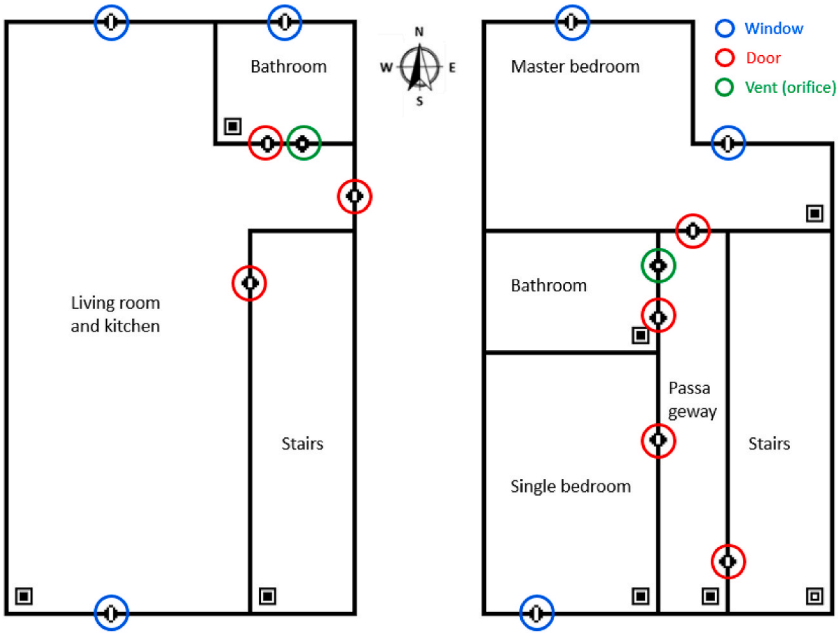

Fig. 1. CONTAM model of the residential building, plan view of the first floor (left) and second floor (right).

Table 2
Apartment windows and corresponding top-hung openings.

	Single bedroom	Master bedroom	Living room & kitchen	Bathroom at first floor
Fixtures (H x W)	Window (1.6 m x 1.5 m)	Window (1.6 m x 1 m) Terrace French door (2.1 m x 0.75 m)	Window (1.6 m x 1 m) Terrace French door (2.1 m x 2 m)	Window (0.4 m x 1.5)
Openable elements (H x W)	Top-hung window (0.6 m x 1.5 m)	Top-hung window (0.6 m x 1 m) Top-hung window (door) (0.5 m x 0.75 m)	Top-hung window (0.6 m x 1 m) Top-hung window (door) (0.5 m x 2 m)	Top-hung window (0.4 m x 1.5 m)

2.3. Dynamic energy model

In Fig. 2, the building energy model developed in TRNSYS is shown. In particular, Fig. 2(a) provides a scheme of the model with the connections between single elements, called Types., whereas Fig. 2(b) illustrates the iterative calculation process occurring at each hourly timestep. The dynamic energy model of the building is developed using TRNBuild, (Type 56). Similarly to CONTAM, each thermal zone presents an air node supposed perfectly mixed in terms of temperature. The zoning criterion for the residential case is the same adopted in CONTAM. Building envelope structures, glazed elements and internal partitions were defined for each zone; the walls separating the housing unit from the adjacent conditioned apartments are considered adiabatic. Concerning the classroom case, one thermal zone is also set in TRNSYS. Time-varying daily schedules were set for the internal heat gains: people, appliances and lights. Table 3 reports the variable presence of people supposed for the apartment rooms, distinguished between workdays and weekend. In the classroom, continuous occupancy of 21 people was considered between 08:00-13:00 and 14:00-16:00, assuming a break at lunchtime, from Monday to Friday. Each person is represented as a 65 W sensible heat gain. In the residential case, a constant internal vapor generation of 0.13 kg/h per person was set, while in the classroom, it was set at 0.085 kg/h. In the first case, a higher latent load from people was chosen to include the typical daily domestic activities that lead to vapor production. The peak value for appliances and lights in the residential building was set at 8 W/m^2 and 2.7 W/m^2, respectively. A constant heat gain from lighting was assumed in the classroom during occupancy hours, equal to 14 W/m^2. All the internal gains were set according to the European Standard EN 16798:2019 [39].

In both case studies, an ideal heating and cooling convective system keeping the indoor air temperature at the desired setpoints was assumed. During the heating season, in the residential building, two-temperature setpoints were set: 21°C during the day (7:00-23:00) and 18°C during the night (23:00-7:00); in the school classroom, a temperature setpoint of 21°C was maintained only for the school day (8:00-16:00), while a setpoint of 18°C was fixed for the rest of the day. During the cooling season, a constant setpoint (26°C for Venice and Rome, 25°C for Helsinki) is set only in the residential case since schools are supposed to stay closed during summer. Instead, free-floating internal temperatures characterize the thermal zones during the mid-seasons. The heating and cooling seasons for the three

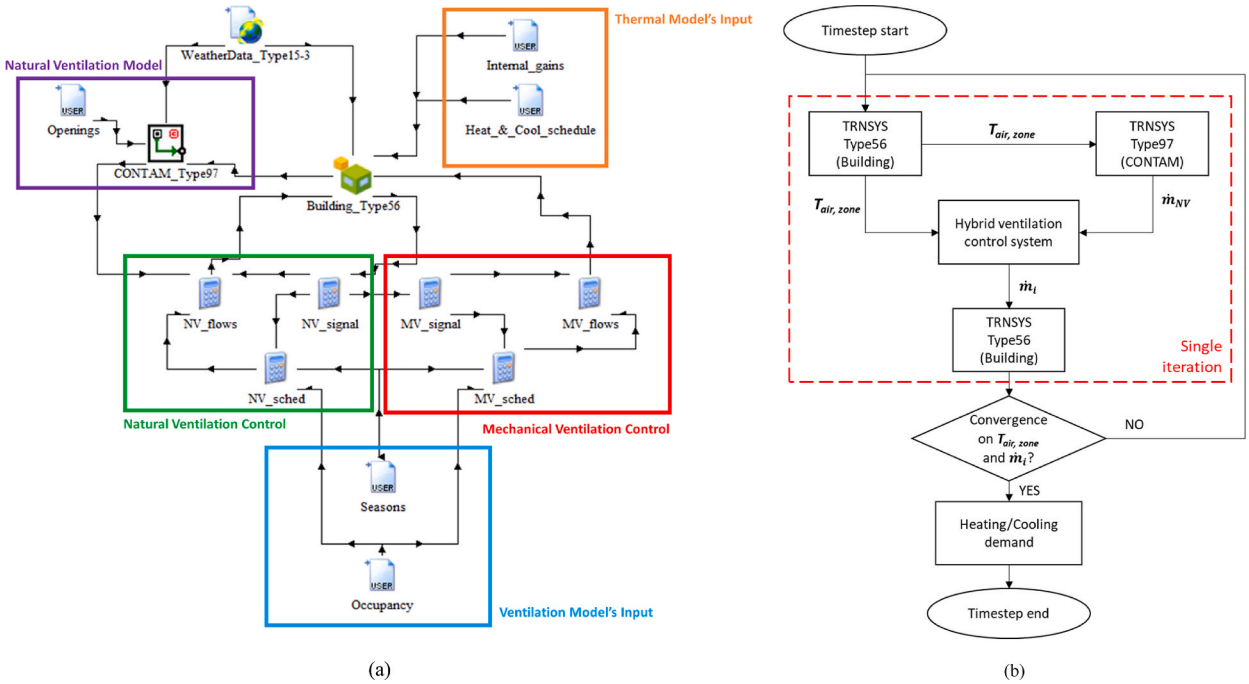

Fig. 2. Building dynamic energy model developed in TRNSYS. Scheme with Types and connections (a). Iterative calculation procedure at each timestep, where $\dot{m}_i$ are natural (NV) or mechanical ventilation (MV) interzonal flow rates based on control system output (b).

Table 3
Occupancy schedule in the residential case.

Number of occupants	Bedrooms		Living room & kitchen		Bathrooms	
	2		4		1	
	Time	Value	Time	Value	Time	Value
Weekday presence (percentage on the number of occupants)	0.00–7.00	100%	7.00–9.00	50%	8.00–9.00	100%
	7.008.00	50%	12.00–13.00	50%	12.00–13.00	100%
	23.00–0.00	100%	17.00–19.00	75%	20.00–22.00	100%
			19.00–23.00	100%		
Weekend presence (percentage on the number of occupants)	0.00–7.00	100%	7.00–9.00	50%	9.00–10.00	100%
	7.00–8.00	50%	9.00–11.00	100%	12.00–13.00	100%
	23.00–0.00	100%	11.00–23.00	50%	18.00–20.00	100%

Table 4
Heating and cooling seasons for each location.

	Heating season	Cooling season	*Notes*
Venice	15th October – 15th April	10th June – 20th September	*Heating season*: from [40]
Rome	1st November – 15th April	10th June – 20th September	*Heating season*: from [40]
Helsinki	1st September – 31st May	1st June – 31st August	*Heating season month*: $T_{avg,\ month} < 15\ ^{\circ}C$ *Cooling season month*: $T_{avg,\ month} \geq 15\ ^{\circ}C$

locations are reported in Table 4.

The coupling between the TRNSYS energy model and CONTAM airflow model is obtained using Type 97. The simulations were carried out with hourly time steps over one year.

2.4. Ventilation and control system

In the two simulated cases, the presence of a hybrid ventilation system is assumed: the indoor spaces are naturally ventilated through the building openings, but when the thermal requirements of the environment are not fulfilled, the switching to a mechanical ventilation system occurs. In the residential case, it provides an air change rate of about 0.5 h^{-1} in the whole housing unit. Each thermal zone is equipped with supply and exhaust diffusers; hence, the supply of fresh air and the extraction of the same exhaust airflow occurs simultaneously in all the building's parts. Table 5 shows the volumetric flow rates set for each zone. On the other hand, in the school classroom case, the criterion of a minimum renewal rate of 4 L/s per student was adopted [39], leading to a total volumetric flow rate of 300 m^3/h. Furthermore, the supply air temperatures follow the setpoint temperatures of the heating and cooling systems. CONTAM was used only for natural ventilation flows, which account for buoyancy and wind effect, while the TRNSYS model provided mechanical ventilation operation. At each simulation timestep, the shift between natural ventilation and mechanical system is driven by a control system based on two control variables: temperatures and occupancy. The difference between indoor and outdoor air temperatures is used as a control strategy to decide whether to keep the windows open, leading to naturally ventilated spaces, or conversely, to activate the fans. If natural ventilation is practicable, only in the occupied zones the windows are kept open to provide air change, according to the occupancy schedules of each room. The flowchart in Fig. 3 outlines the overall control strategy adopted in this work for the residential case.

As illustrated in the figure, different limit temperature differences are used for exploiting natural ventilation depending on the current season. In particular, an upper limit on the external temperature is chosen as a threshold value to open or close the windows during the cooling season. For each case study, the control parameters were varied in order to obtain three sets of threshold values for the simulation of three scenarios.

- a baseline configuration (Case A);
- a natural ventilation dominant configuration (Case B);
- a mechanical ventilation dominant configuration (Case C).

In Case B and C, temperature controls are modified to obtain longer natural and mechanical ventilation periods, respectively, compared to the baseline (Case A). Overall, 18 different situations are simulated (three scenarios for two building types in three locations); the values of the control parameters are reported for each one in Table 6.

For each scenario, an iterative procedure has been implemented to adjust the opening area of the top-hung windows at the

Table 5
Mechanical ventilation flow rates in the apartment rooms.

	Single bedroom	Master bedroom	Living room & kitchen	First floor Bathroom	Second floor bathroom
Volumetric flowrate [m^3/h]	12	18	80	20	30
ACH [h^{-1}]	0.52	0.59	0.98	2.04	2.34

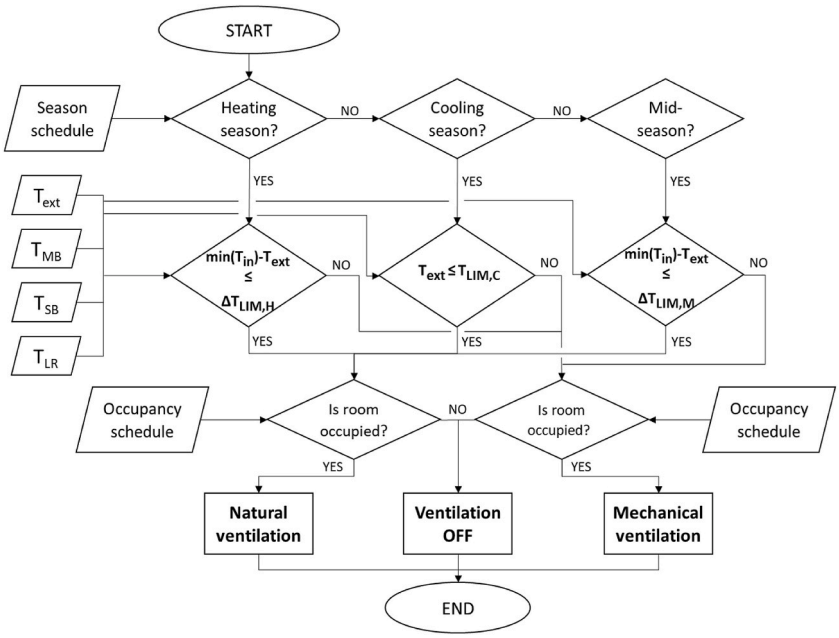

Fig. 3. Flowchart of ventilation control strategy for the apartment (MB=Master bedroom, SB=Single bedroom, LR=Living room, H=Heating season, C=Cooling season, M=Mid-season).

Table 6
Control parameters values for each case study.

Case study	Climate	Configuration	$\Delta T_{LIM,\ H}$ [°C]	$\Delta T_{LIM,\ M}$ [°C]	$T_{LIM,\ C}$ [°C]
Residential building	Helsinki	Baseline	10	-	25
		NV dominant	15	-	27
		MV dominant	5	-	20
	Venice	Baseline	5	6	26
		NV dominant	10	10	28
		MV dominant	0	0	22
	Rome	Baseline	5	6	26
		NV dominant	10	10	28
		MV dominant	0	0	22
School classroom	Helsinki	Baseline	12	–	–
		NV dominant	16	–	–
		MV dominant	5	–	–
	Venice	Baseline	10	10	–
		NV dominant	15	15	–
		MV dominant	0	0	–
	Rome	Baseline	10	10	–
		NV dominant	15	15	–
		MV dominant	0	0	–

timesteps of natural ventilation. Starting from the first attempt values for the percentage of open area of the elements, a calibration was carried out in order to maintain the natural ventilation flow rates within the established range of air change rates according to room end-use: $2 \div 4\ h^{-1}$ for bathrooms, $1 \div 2\ h^{-1}$ for living room, $0.5 \div 2\ h^{-1}$ for bedrooms, and $2 \div 4\ h^{-1}$ for the classroom. Without this procedure, excessively high flow rates would arise, especially in the heating season when the stack effect becomes quite intense.

2.5. Energy demand and risk calculation

The evaluation of the hybrid ventilation systems and the comparison between the different control configurations among the analysed case studies were made in terms of thermal and electrical energy demand and airborne infection risk from COVID-19.

2.5.1. Thermal energy calculation

The thermal energy used in the different scenarios was calculated, assuming the presence in all the case studies of an ideal convective heating system and a mechanical ventilation unit. The ideal system was used to maintain the setpoint temperature inside the building, and the energy required by the system was determined through the simulations of the above-described model. The energy demand necessary to fill the temperature decrease or increase due to air infiltration in naturally ventilated hours is included in TRNSYS

simulations. On the other hand, when mechanical ventilation unit works, it brings the outdoor air directly from the external conditions to the desired supply temperature and relative humidity, performing specific processes.

The calculation of thermal (sensible and latent) energy for air handling depends on the season of operation. In heating conditions, outdoor air is sucked by the supply fan, and after the filtering process, it undergoes heat recovery from exhaust air – through a cross-flow heat exchanger with an efficiency of 0.9. Then, the processes of sensible heating (through the pre-heating coil), saturation (in an adiabatic saturator with efficiency 0.9) and post-heating take air to the supply conditions (e.g., 18 or 21°C and 50% RH, see Section 2.3). In Eq. (1), the calculation of the energy use for air handling in the heating season ($q_{AH,H}$) is shown:

$$q_{AH,H} = \dot{m}_{air}\Delta h_{preH} + \dot{m}_{air}\Delta h_{postH} \tag{1}$$

where $\dot{m}_{air}$ is the air mass flowrate, Δh_{preH} and Δh_{postH} are the differences of air enthalpy between the inlet and outlet of the pre-heating and post-heating coil, respectively.

In the cooling season, the mechanical ventilation unit layout is different, and air undergoes two transformations: cooling and dehumidification through a cooling coil and the post-heating process to reach the supply conditions, which are 26°C (25°C for Helsinki) and 50% of RH in cooling mode. The energy use for air handling in summer is presented separating the sensible and latent components, which are calculated according to Eqs. (2) and (3), respectively:

$$q_{AH,cool,sens} = \dot{m}_{air}\Delta T_{CD} * \left(c_{p,da} + x_v c_{p,v}\right) \tag{2}$$

$$q_{AH,cool,lat} = \dot{m}_{air}\Delta x_{CD} r_{0,w} \tag{3}$$

where $c_{p,da}$ is the dry air specific heat (1006 J/(kg K)), $c_{p,v}$ is the vapor specific heat (1875 J/(kg K)), $r_{0,w}$ is the latent heat of vaporization of water at 0°C (2501 kJ/kg), Δx_{CD} and ΔT_{CD} are the differences between the inlet and outlet of the cooling coil of specific humidity and air temperature, respectively.

The seasonal heating and cooling (sensible and latent) demand (E_{AH}) are determined for all the analysed scenarios, through the sum of the energy calculated for each timestep:

$$E_{AH,i} = \sum_j q_{AH,i,j}\tau_j \tag{4}$$

where i is the energy component (e.g., heating, cooling-sensible, cooling-latent), j is the simulation timestep and τ is its length.

2.5.2. Electrical energy calculation

The electrical consumption for air handling was calculated, assuming the pressure losses at the nominal airflow rate of the corresponding case study for each component. The overall pressure losses value was therefore interpolated with the characteristic curve of the fan, revealing the working point used for calculating the fan power. The annual electrical consumption ($E_{AH,el}$) was determined for all the analysed scenarios, through the sum of the energy calculated for each timestep when the mechanical ventilation is active:

$$E_{AH,el} = \sum_j q_{AH,el,j}\tau_j \tag{5}$$

where $q_{AH,el,j}$ is the sum of the exhaust and supply fan power for each timestep, j is the simulation timestep and τ is its length.

2.5.3. Airborne infection risk calculation

The airborne infection risk from COVID-19 was calculated over one reference day. In the residential case, it was evaluated only in the living room during the weekend, when this zone is more occupied during the daytime. For both cases, the presence of one asymptomatic subject was assumed and the individual infection probability was assessed by applying the Wells-Riley model. The infectious aerosols are expressed in terms of quanta, a hypothetical dose unit that makes 63.2% of an exposed population sick [41]. The quanta exhalation rate of the infected source is specific for the considered disease and depends on the activity level. In both cases, a quanta concentration balance was set with the assumption of a well-mixed room, as expressed by Eq. (6):

$$\frac{dC}{dt} = \frac{ER * I}{V} - (ACH + k + \lambda) * C \tag{6}$$

where C is the quanta concentration, ER is quanta generation rate for the disease, I is the number of infected sources, V is room volume, ACH is room air changes per hour, k and λ represent the loss terms related to virus particle gravitational deposition and viral inactivation, respectively. Values of 0.24 h^{-1} for k and 0.63 h^{-1} for λ were fixed according to Ref. [42]. It was assumed that outdoor air does not contain infectious quanta, and aerosol recirculation from adjacent zones in the residential building was neglected. Quanta concentration represents the virus-laden material available at the breathing zone of a susceptible subject, whose infection risk is calculated through the exponential probability relationships expressed by Eq. (7):

$$P_I = 1 - \exp\left(-p\int C(t)dt\right) \tag{7}$$

where p is the breathing flow rate of the susceptible person. The exponent represents the intake dose and is given by an integral of

quanta concentration over the exposure time. Supposing that in both case studies the subjects involved in risk assessment usually perform intermediate activities between sedentary level and light exercise, a breathing flow rate of 0.60 m^3/h and an emission rate of 30 quanta/h for COVID-19 were chosen in compliance with [43]. The Wells-Riley model is based on two assumptions, namely room perfect mixing and steady-state quanta concentration. The former is preserved for the apartment's living room and school classroom in compliance with multi-zone modelling approach, whereas the quanta concentration is calculated at each timestep discretizing Eq. (6), and the obtained value is used to calculate the inhaled dose on the current timestep. Then, the cumulated dose from the start of exposure is used to estimate the airborne infection risk through Eq. (7).

3. Results and discussion

For each case study, residential building and classroom, the effect of the control strategy (baseline, NV dominant, MV dominant) adopted for the hybrid ventilation system is analysed and a comparison is carried out in terms of the operating time of natural and mechanical ventilation, heating and cooling energy demand, fans' electrical absorption when the mechanical ventilation is on, and infection risk extent.

In Fig. 4, natural and mechanical ventilation operating time is reported in terms of the percentage of the total hours of building usage over the year for the apartment (a) and the classroom (b). In the residential unit (Fig. 4(a)), the effect of the control strategy implemented in the model is clear. In Rome and Venice, in the baseline situation (Case A), the building is naturally ventilated for almost half the time compared to mechanical ventilation operation, while in NV dominant scenario (Case B), the natural ventilation

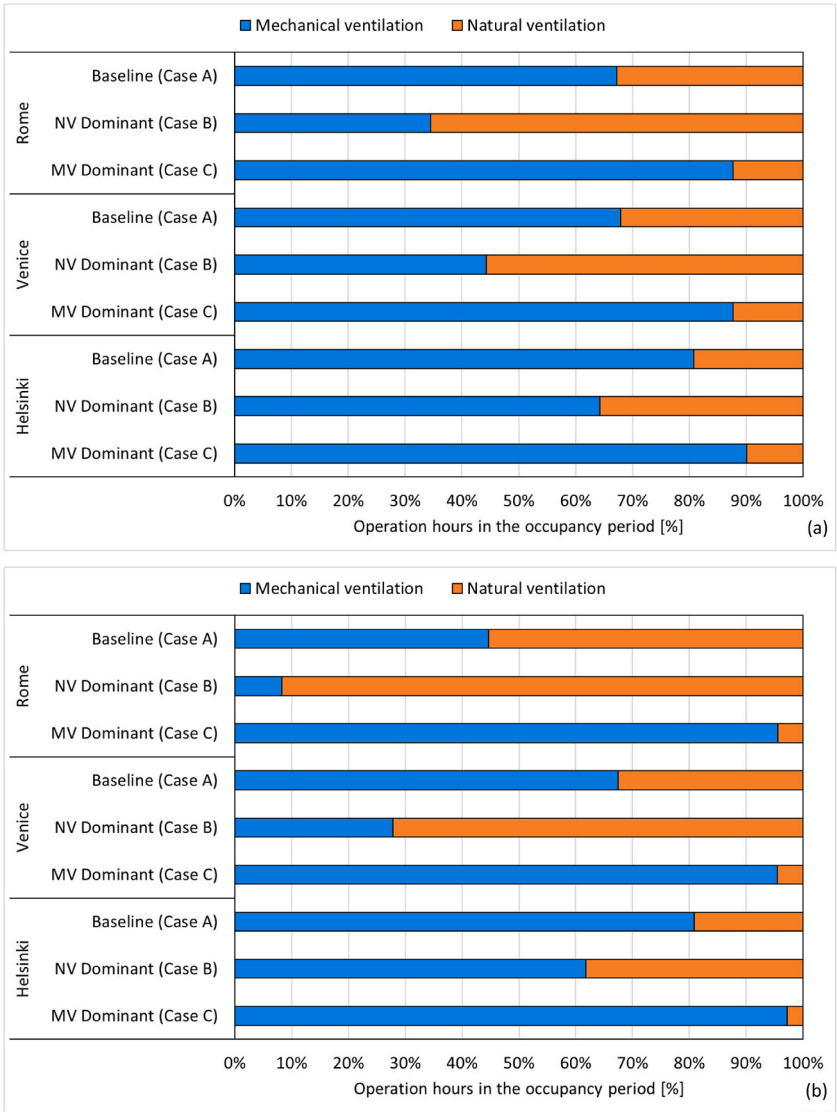

Fig. 4. Natural and mechanical ventilation operation time during the occupancy period for the residential apartment (a) and the school classroom (b).

hours increase by about two times. The opposite situation occurs for MV dominant system (Case C), with a halving of natural ventilation hours compared to the base case. In Helsinki, the building is mainly mechanically ventilated during the year, from a minimum of 64% of the time in Case B to a maximum of 90% in Case C, due to lower external temperatures; therefore, the threshold values for the control of natural ventilation (see Table 6) are less frequently met in the heating and mid-season.

A similar trend can be observed in the school classroom (Fig. 4(b)). Compared to the apartment case, the share of natural ventilation hours during the operative period is higher because the classroom is occupied during the central and warmer hours of the day, and looser control limits are set to open the windows (see Table 6). Comparing the baseline and NV dominant scenarios, it can be noticed that natural ventilation is more frequent in Rome given the warmer climate than Venice and Helsinki, therefore, the control thresholds are more easily met. In the MV dominant scenario, mechanical ventilation is active for more than 95% in all the locations.

The heating and cooling energy needs have been determined for the apartment considering the net heated and cooled floor area (see Table 1). Concerning the heating demand, results are divided into convective system output (TRNSYS outcome) and energy required for air handling when the building is mechanically ventilated. The results for the apartment are shown in Fig. 5. For a given location, the overall heating demand remains almost the same between the various scenarios; the climate effect can be observed with a maximum annual heating demand of 2598 kWh in Rome, 3762 kWh in Venice and 6948 kWh in Helsinki. The difference lies in the different allocation of the energy demand: in NV dominant configurations, the convective system accounts for about two times compared to air handling processes. This means that with this control strategy scenario, the primary system works for more time and its thermal capacity has to be set accordingly. On the contrary, the share of the air handling energy need increases in Case A and C. In Rome, the convective system and the heating coils in the mechanical ventilation unit account for the same share in these two scenarios (i.e., 49%–51%, Case A), whereas the convective contribution increases in Venice (i.e., 58%–42%, Case A) and in Helsinki (i.e., 63%–37%, Case A).

The outcomes for the classroom are reported in Fig. 6. The climate influence is still highlighted by the maximum annual demand (854 kWh in Rome, 1126 kWh in Venice and 2369 kWh in Helsinki). It can be noticed that the overall energy demand is higher in the MV dominant scenarios, especially in Rome. This is due to the fact that the classroom is well-insulated and internal heat gains contribute to heating the space during the season.

Fig. 7 illustrates the fans' electrical absorption during the heating season for the apartment and the school classroom. In the residential case, as expected, a substantial decrease in electrical consumption is achieved moving from Case C to B, with savings reaching 40% in Rome, 22% in Venice and 30% in Helsinki. In contrast, the consumptions are similar between Case A and C, meaning that in those scenarios, the operating hours of mechanical ventilation are almost equal in the heating season. In the school classroom case, the demand reduction from Case C to B is remarkable, up to 86% in Rome, 58% in Venice, 37% in Helsinki. The energy demand also decreases from Case C to A since mechanical ventilation hours are lower in the second case (given the higher temperature differences set for providing natural ventilation, see Table 6).

The cooling energy demand is highlighted in Fig. 8(a) only for the apartment case since school is not occupied during summer. A subdivision into sensible and latent cooling is provided, given the importance of dehumidification during the cooling season. Both sensible and latent shares are given by the sum of the convective system and mechanical ventilation unit contributions. A significant reduction in the annual sensible cooling demand is obtained moving from MV to NV dominant scenario (by 24% kWh in Rome, 31% in Venice, 11% in Helsinki). The same effect can be seen for the latent share only in Rome and Venice (30% in Rome, 29% in Venice), whereas it remains the same among the scenarios in Helsinki due to the favourable external conditions in terms of humidity. The total cooling demand is almost the same for Venice and Rome, the former presenting a higher latent share, the latter a higher sensible share.

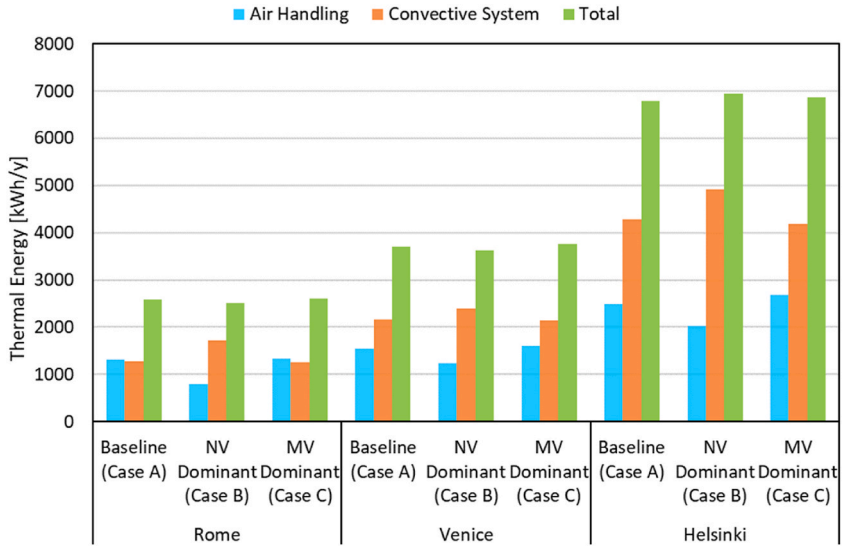

Fig. 5. Heating demand for air handling and the ideal heating system in the residential apartment case study.

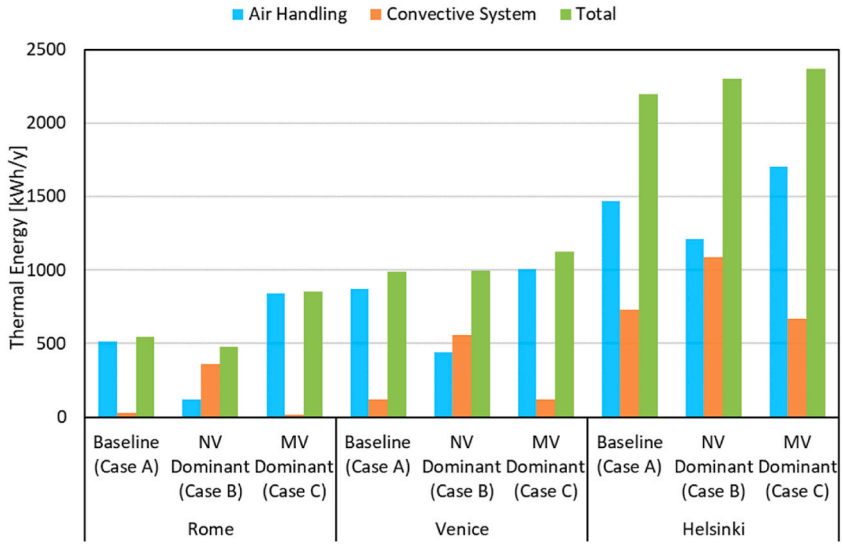

Fig. 6. Heating demand for air handling and the ideal heating system in the school classroom case study.

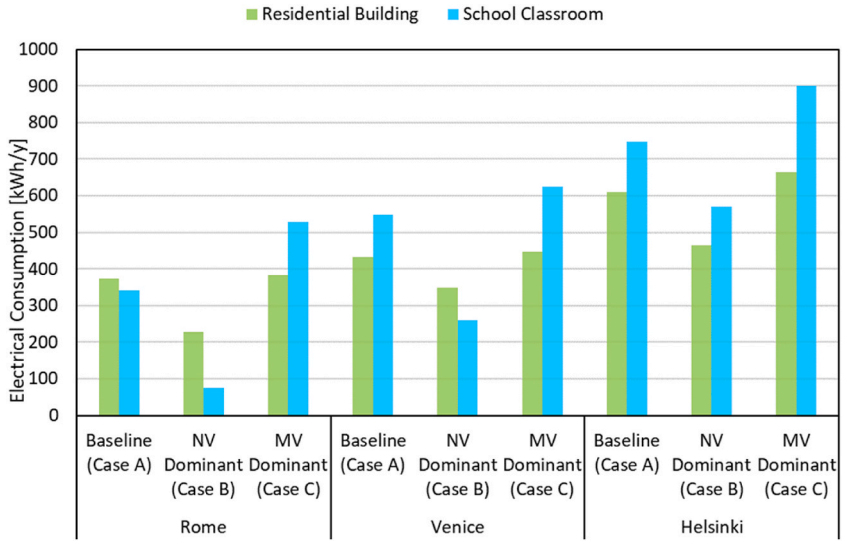

Fig. 7. Electrical consumption for air handling in the residential apartment and the school classroom during the heating season.

On the other hand, the total cooling demand in Helsinki is about half that of the two Italian cities.

In Fig. 8(b), the apartment's electrical consumption for air handling in the cooling season is reported. In Helsinki, the flat is naturally ventilated for most of the season in all control scenarios, with an annual maximum of 26 kWh in Case C. In Rome and Venice, a gradual decrease is obtained, moving from Case C to A and B, highlighting a corresponding increase in the natural ventilation hours. The maximum savings amount to 69% in Rome and 84% in Venice.

The risk assessment was carried out assuming that involved subjects do not wear protective devices and masks. In the residential building, risk has been evaluated in the living room during a day on the weekend when the room is occupied most of the daytime. Three specific days, one for each season were chosen, and risk was calculated in the baseline, NV dominant and MV dominant situations during these days. The risk was assessed for typical school days for the classroom, one from the heating season and two from the mid-season. Since quanta concentration balance and infection probability are affected only by the ventilation flow rate, only the results obtained for Venice are shown, being those for the other locations similar. Figs. 9 and 10 show the trends of infection risk and air changes per hour for the residential building and the school classroom, respectively. When the room is not occupied, the infection risk remains constant because it only depends on how much infectious material the susceptible subject has previously inhaled. It is evident that the higher the ventilation rate on average during the day, the lower the infection probability for the susceptible subjects. In particular, when the renewal flow rate increases, the risk curve becomes less steep and tends to flatten. If the ventilation rate rises, the

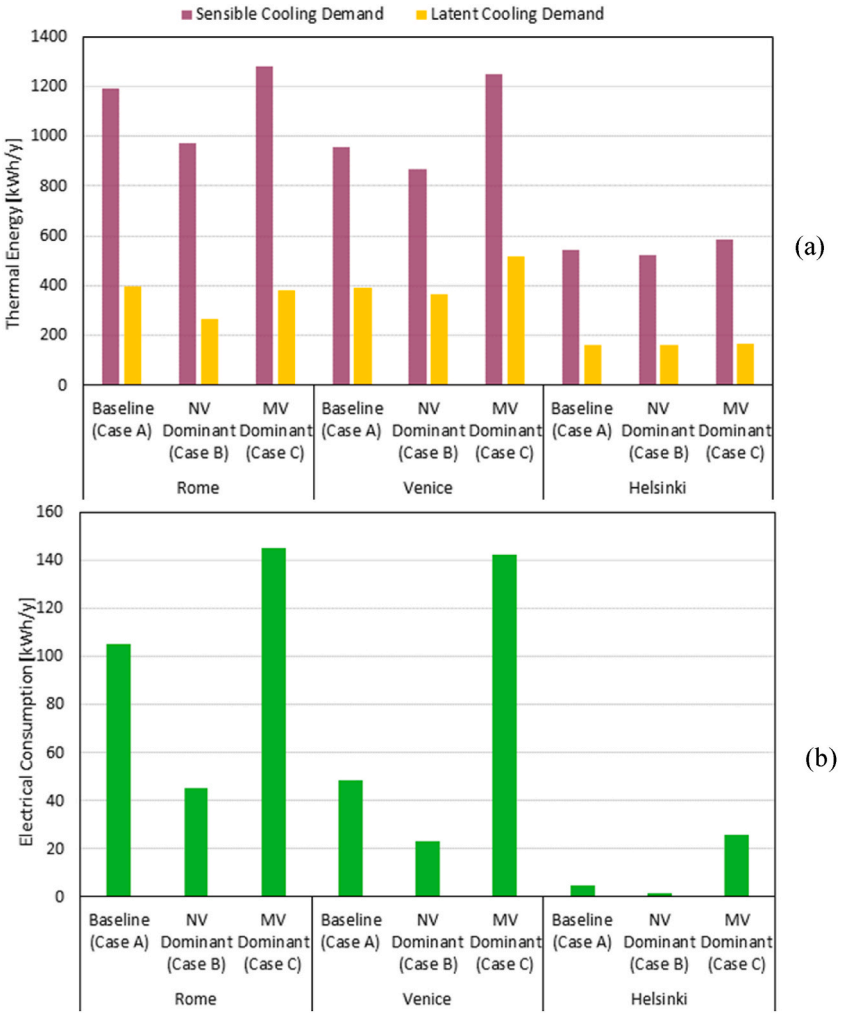

Fig. 8. Sensible and latent cooling demand (a) and electrical consumption for air handling (b) during the cooling season for the apartment.

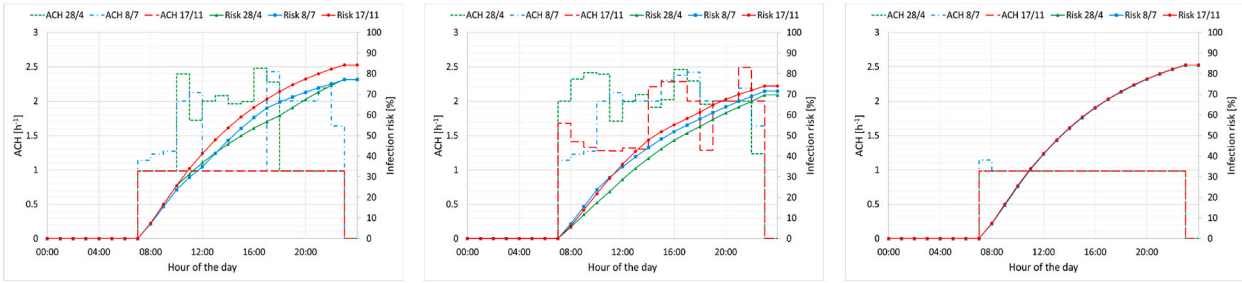

(a) (b) (c)

Fig. 9. Infection risk trends for the apartment in Venice. Baseline – Case A (a). NV dominant – Case B (b). MV dominant – Case C (c).

dilution and the removal of virus-laden aerosol from the room enhance. In the apartment, the worst situation is the MV dominant situations, due to the lower air changes per hour. In this case, the infection risk reaches almost 85%. The NV dominant situation is the best solution with higher ventilation rates during the day that result in an infection risk below 70%, though still pretty high. In the baseline, days of both ventilation modes often could occur, leading to intermediate risk values. A similar situation can be observed for the classroom. The best situation is represented by NV dominant system with an infection risk between 18 and 23%, while the worst is with MV dominant system, where the infection risk reaches a value of 24%. Risk extent is lower than that in the apartment's living

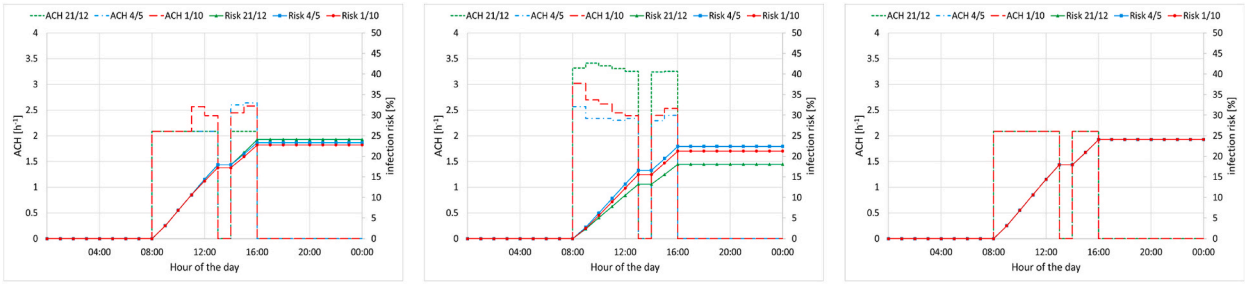

(a) (b) (c)

Fig. 10. Infection risk trends for the school classroom in Venice. Baseline – Case A (a). NV dominant – Case B (b). MV dominant – Case C (c).

room due to the larger room volume that ensures higher dilution of infectious aerosols.

Eventually, it can be observed that in MV dominant situations (Case C), the infection risk reaches the largest values because the ventilation flow rates are lower compared to the other cases. To get the same risk mitigation as in the NV dominant system (Case B), the supply flow rates should be increased to match those achievable through natural ventilation with envelope openings. This operation will certainly increase the energy demand for air handling, thus promoting well-controlled natural ventilation would be convenient both in terms of energy savings and risk mitigation.

4. Conclusions

In the present paper, the energy demand and infection risk evaluation of a hybrid ventilation system has been carried out for two different building types, a residential building and a school classroom. The evaluation of ventilation control strategies is a complex issue and performing it with measurements is difficult, especially over long periods of time. For this reason, a simulation approach based on dynamic building models was adopted by coupling two already validated and well-established software, CONTAM and TRNSYS. The airflow network was created in CONTAM to determine natural ventilation flows between thermal zones and infiltrations from the external environment. The transient thermal model for calculating the building heating and cooling loads was built in TRNSYS. The annual simulations were carried out with hourly time step, considering three locations with different climatic conditions: Rome, Venice and Helsinki. A control strategy was adopted to regulate the switch between ventilation modes based on two variables: external temperature and occupancy. Three scenarios were implemented to analyse different control configurations: a baseline case, a natural ventilation dominant case and a mechanical ventilation dominant case. The following results emerged from this study.

- For the apartment, in all locations, overall heating demand remains almost the same between different control scenarios. In NV dominant scenario, the convective system contribution is two times that required for air handling in mechanical ventilation mode, meaning that the operating hours of the primary systems increases and its thermal capacity has to be set accordingly. For baseline and MV dominant scenarios, the convective system share increases from 49% in Rome to 63% in Helsinki.
- Moving from MV to NV dominant scenarios, sensible cooling demand significantly decreases, e.g., by 24% kWh in Rome, 31% in Venice and 11% in Helsinki. Latent cooling demand undergoes a relevant reduction in Rome (30%) and Venice (29%), while it remains almost the same in Helsinki. The total cooling demand is similar between Venice and Rome and two times that of Helsinki.
- In the heating season, fan electrical absorption significantly decreases if the operating hours are strongly reduced from MV to NV dominant scenario. Savings of 40% in Rome, 22% in Venice and 30% in Helsinki are obtained in the residential case. In the classroom case, they are up to 86% in Rome, 58% in Venice, 37% in Helsinki.
- In the cooling season, in the apartment case, the electrical energy consumption of the fan is low in Helsinki (maximum of 26 kWh/year in MV dominant scenario). In Rome and Venice, maximum savings of 69% and 84%, respectively, are achieved going from MV to NV dominant scenario.
- NV dominant cases involve higher ventilation flow rates than MV dominant ones, with benefits in terms of risk mitigation. A reduction from 85% to 70% is achieved in the apartment and from 25% to 18% in the classroom.
- The mechanical system should supply higher flow rates to reach the same risk mitigation, leading to an increase in both fan electrical absorption and heating and cooling demand at the heating and cooling coils, respectively. Therefore, well-controlled hybrid ventilation that promotes natural ventilation could be convenient for maintaining healthy indoor spaces while saving energy.

The presented work raises some limitations and needs further improvements. The comparison between different scenarios is carried out in terms of net energy demand for heating and cooling purposes; however, it would be interesting to consider the efficiency of typical building HVAC plants to evaluate the actual final consumptions and primary energy request, accordingly.

Authors contribution

Giacomo Tognon: Conceptualization, Methodology, Software, Data Curation, Writing - Original Draft, Writing - Review & Editing. **Marco Marigo:** Conceptualization, Methodology, Software, Data Curation, Writing - Original Draft, Writing - Review & Editing.

Michele De Carli: Supervision. **Angelo Zarrella:** Conceptualization, Methodology, Supervision, Writing - Review & Editing, Project administration.

Declaration of competing interest

The authors declare that they have no known competing financial interests or personal relationships that could have appeared to influence the work reported in this paper.

Data availability

Data will be made available on request.

References

[1] Eurostat, Energy data 2020 edition: statistical book. https://ec.europa.eu/eurostat/databrowser/view/ten00124/default/table?lang=en. (Accessed 15 January 2023).
[2] World Health Organization, Coronavirus disease (COVID-19), How is it transmitted?. https://www.who.int/news-room/questions-and-answers/item/coronavirus-disease-covid-19-how-is-it-transmitted. (Accessed 15 January 2023).
[3] K. Ram, R.C. Thakur, D.K. Singh, et al., Why airborne transmission hasn't been conclusive in case of COVID-19? An atmospheric science perspective, Sci. Total Environ. 773 (2021), 145525, https://doi.org/10.1016/j.scitotenv.2021.145525.
[4] P. Cheng, K. Luo, S. Xiao, et al., Predominant airborne transmission and insignificant fomite transmission of SARS-CoV-2 in a two-bus COVID-19 outbreak originating from the same pre-symptomatic index case, J. Hazard Mater. 425 (2022), https://doi.org/10.1016/j.jhazmat.2021.128051.
[5] L. Stabile, A. Pacitto, A. Mikszewski, L. Morawska, G. Buonanno, Ventilation procedures to minimize the airborne transmission of viruses in classrooms, Build. Environ. 202 (2021), https://doi.org/10.1016/j.buildenv.2021.108042.
[6] F. Cheng, C. Cui, W. Cai, X. Zhang, Y. Ge, B. Li, A novel data-driven air balancing method with energy-saving constraint strategy to minimize the energy consumption of ventilation system, Energy 239 (2022), https://doi.org/10.1016/j.energy.2021.122146.
[7] International Energy Agency (IEA), Control Strategies for Hybrid Ventilation in New and Retrofitted Office and Educational Buildings (HYBVENT), Annex 35 - Technical Synthesis Report, 2006.
[8] H.C. Burridge, S. Bontitsopoulos, C. Brown, et al., Variations in classroom ventilation during the COVID-19 pandemic: insights from monitoring 36 naturally ventilated classrooms in the UK during 2021, J. Build. Eng. 63 (2023), 105459, https://doi.org/10.1016/j.jobe.2022.105459.
[9] W. Li, Q. Chen, Design-based natural ventilation cooling potential evaluation for buildings in China, J. Build. Eng. 41 (2021), 102345, https://doi.org/10.1016/j.jobe.2021.102345.
[10] M.Á. Navas-Martín, T. Cuerdo-Vilches, Natural ventilation as a healthy habit during the first wave of the COVID-19 pandemic: an analysis of the frequency of window opening in Spanish homes, J. Build. Eng. 65 (2023), https://doi.org/10.1016/j.jobe.2022.105649.
[11] Y. Peng, Y. Lei, Z.D. Tekler, N. Antanuri, S.K. Lau, A. Chong, Hybrid system controls of natural ventilation and HVAC in mixed-mode buildings: a comprehensive review, Energy Build. 276 (2022), https://doi.org/10.1016/j.enbuild.2022.112509.
[12] P. Kumar, S. Hama, R.A. Abbass, et al., CO2 exposure, ventilation, thermal comfort and health risks in low-income home kitchens of twelve global cities, J. Build. Eng. 61 (2022), 105254, https://doi.org/10.1016/j.jobe.2022.105254.
[13] L. Ledo Gomis, M. Fiorentini, D. Daly, Potential and practical management of hybrid ventilation in buildings, Energy Build. 231 (2021), https://doi.org/10.1016/j.enbuild.2020.110597.
[14] J. Chen, G. Augenbroe, X. Song, Evaluating the potential of hybrid ventilation for small to medium sized office buildings with different intelligent controls and uncertainties in US climates, Energy Build. 158 (2018) 1648–1661, https://doi.org/10.1016/j.enbuild.2017.12.004.
[15] H. Cho, D. Cabrera, S. Sardy, R. Kilchherr, S. Yilmaz, M.K. Patel, Evaluation of performance of energy efficient hybrid ventilation system and analysis of occupants' behavior to control windows, Build. Environ. 188 (2021), https://doi.org/10.1016/j.buildenv.2020.107434.
[16] C. Vallianos, A. Athienitis, J. Rao, Hybrid ventilation in an institutional building: modeling and predictive control, Build. Environ. 166 (2019), https://doi.org/10.1016/j.buildenv.2019.106405.
[17] C.C. Menassa, N. Taylor, J. Nelson, A framework for automated control and commissioning of hybrid ventilation systems in complex buildings, Autom. ConStruct. 30 (2013) 94–103, https://doi.org/10.1016/j.autcon.2012.11.022.
[18] B.D. Less, S.M. Dutton, I.S. Walker, M.H. Sherman, J.D. Clark, Energy savings with outdoor temperature-based smart ventilation control strategies in advanced California homes, Energy Build. 194 (2019) 317–327, https://doi.org/10.1016/j.enbuild.2019.04.028.
[19] K.Y. Park, D.O. Woo, S.B. Leigh, L. Junghans, Impact of hybrid ventilation strategies in energy savings of buildings: in regard to mixed-humid climate regions, Energies 15 (2022), https://doi.org/10.3390/en15061960.
[20] N. Vadamalraj, K. Zingre, S. Seshadhri, P. Arjunan, S. Srinivasan, Hybrid ventilation system and soft-sensors for maintaining indoor air quality and thermal comfort in buildings, Atmosphere 11 (2020), https://doi.org/10.3390/ATMOS11010110.
[21] A. O' Donovan, P.D. O' Sullivan, The impact of retrofitted ventilation approaches on long-range airborne infection risk for lecture room environments: design stage methodology and application, J. Build. Eng. 68 (2023), 106044, https://doi.org/10.1016/j.jobe.2023.106044.
[22] R. Stasi, F. Ruggiero, U. Berardi, The efficiency of hybrid ventilation on cooling energy savings in NZEBs, J. Build. Eng. 53 (2022), 104401, https://doi.org/10.1016/j.jobe.2022.104401.
[23] S.A. Klein, W.A. Beckman, J.W. Mitchell, et al., Trnsys 17 (2009) 1–29, 5.
[24] W.S. Dols, B.J. Polidoro, CONTAM User Guide and Program Documentation, 2015, https://doi.org/10.6028/NIST.TN.1887. Version 3.2, Gaithersburg, MD.
[25] B.F. Goldiez, Validation of a Transient Simulation Program (TRNSYS), Retrospective Theses and Dissertations, 1979, p. 417. https://stars.library.ucf.edu/rtd/417. (Accessed 22 May 2023).
[26] F. Haghighat, A. Megri, A comprehensive validation of two airflow models - COMIS and CONTAM, Indoor Air 6 (1996) 278–288.
[27] I. Khalifa, L. Gharbi Ernez, E. Znouda, C. Bouden, Coupling TRNSYS 17 and CONTAM: simulation of a naturally ventilated double-skin façade, Adv. Build. Energy Res. 9 (2015) 293–304, https://doi.org/10.1080/17512549.2015.1050694.
[28] W.S. Dols, S.J. Emmerich, B.J. Polidoro, Using coupled energy, airflow and indoor air quality software (TRNSYS/CONTAM) to evaluate building ventilation strategies, Build. Serv. Eng. Res. Tecnol. 37 (2016) 163–175, https://doi.org/10.1007/s12273-016-0279-2.
[29] T.P. McDowell, S. Emmerich, J.W. Thornton, G. Walton, Integration of airflow and energy simulation using CONTAM and TRNSYS, Build. Eng. 109 (2003) 757–770, part 2.
[30] Y. Wen, S.K. Lau, J. Leng, K. Liu, Sustainable underground environment integrating hybrid ventilation, photovoltaic thermal and ground source heat pump, Sustain. Cities Soc. 90 (2023), https://doi.org/10.1016/j.scs.2022.104383.
[31] C.F. Picard, L. Cony Renaud Salis, M. Abadie, Home quarantine: a numerical evaluation of SARS-CoV-2 spread in a single-family house, Indoor Air 32 (2022), https://doi.org/10.1111/ina.13035.
[32] T. Pistochini, C. Mande, S. Chakraborty, Modeling impacts of ventilation and filtration methods on energy use and airborne disease transmission in classrooms, J. Build. Eng. 57 (2022), 104840, https://doi.org/10.1016/j.jobe.2022.104840.
[33] W.F. Wells, Airborne Contagion and Air Hygiene. An Ecological Study of Droplet Infections, Harvard University Press, 1955.

[34] E.C. Riley, G. Murphy, R.L. Riley, Airborne spread of measles in a suburban elementary school, Am. J. Epidemiol. 107 (1978) 421–432, https://doi.org/10.1093/oxfordjournals.aje.a112560.
[35] President of the Italian Republic, D. Lgs 19 August 2005, N. 192: "Attuazione Della Direttiva 2002/91/CE Relativa Al Rendimento Energetico Nell'edilizia". ([In Italian]).
[36] Energyplus, Weather data. https://energyplus.net/weather. (Accessed 15 January 2023).
[37] J. Shaeri, M. Mahdavinejad, M.H. Pourghasemian, A new design to create natural ventilation in buildings: wind chimney, J. Build. Eng. 59 (2022), 105041, https://doi.org/10.1016/j.jobe.2022.105041.
[38] M.V. Swami, S. Chandra, Correlations for pressure distribution on buildings and calculation of natural-ventilation airflow, Build. Eng. 94 (1988) 243–266.
[39] European Committee for Standardization, Energy Performance of Buildings — Assessment of Overall Energy Performance, 2019. EN 16798-1.
[40] President of the Italian Republic, DPR 29 august 1993, n. 412: "Regolamento recante norme per la progettazione, l'installazione, l'esercizio e la manutenzione degli impianti termici degli edifici ai fini del contenimento dei consumi di energia". ([In Italian]).
[41] G.N. Sze To, C.Y.H. Chao, Review and comparison between the Wells-Riley and dose-response approaches to risk assessment of infectious respiratory diseases, Indoor Air 20 (2010) 2–16, https://doi.org/10.1111/j.1600-0668.2009.00621.x.
[42] G. Buonanno, L. Morawska, L. Stabile, Quantitative assessment of the risk of airborne transmission of SARS-CoV-2 infection: prospective and retrospective applications, Environ. Int. 145 (2020), 106112, https://doi.org/10.1016/j.envint.2020.106112.
[43] L. Schibuola, C. Tambani, High energy efficiency ventilation to limit COVID-19 contagion in school environments, Energy Build. 240 (2021), 110882, https://doi.org/10.1016/j.enbuild.2021.110882.